AIAA Meeting Papers on Disc, June 1996
A9636512, DAAH04-95-20003, DAAH04-95-C0008, AIAA Paper 96-2060

Effect of chemical reactions on the decay of isotropic homogeneous turbulence

M. P. Martin Aguirre
Minnesota Univ., Minneapolis

Graham V. Candler
Minnesota Univ., Minneapolis

AIAA, Fluid Dynamics Conference, 27th, New Orleans, LA, June 17-20, 1996

Direct numerical simulations (DNS) are used to simulate the decay of an isotropic, turbulent, chemically-reacting flow at high temperatures. The independent parameters that govern the physical process are introduced. The different effects from each of the parameters in the flow are explained by using the results from the DNS. It is found that there is a feedback mechanism between the chemical reactions and the turbulent motion. This feedback is positive for exothermic reactions and negative for endothermic reactions. (Author)

AIAA 96-2060

Effect of Chemical Reactions on the Decay of Isotropic Homogeneous Turbulence

M. Pino Martín Aguirre
Graham V. Candler
Department of Aerospace Engineering and Mechanics.
University of Minnesota, Minneapolis MN 55455

Abstract

Direct numerical simulations, (DNS), are used to simulate the decay of an isotopic, turbulent, chemically-reacting flow at high temperatures. The independent parameters that govern the physical process are introduced. The different effects from each of the parameters in the flow are explained by using the results from the DNS. It is found that there is a feedback mechanism between the chemical reactions and the turbulent motion. This feedback is positive for exothermic reactions and negative for endothermic reactions.

I. Introduction

The research[1] conducted In flows such as hypersonic boundary layers, where the flow is turbulent, reacting, and the temperatures are up to 10,000 K, the rate of reaction is determined by the temperature. To accurately model this type of flow, one of the issues that must be addressed is the understanding of the physical phenomena driving the interaction between the chemical reactions and the turbulent motion, and the behavior of the nearly universal small scales.

Because the reaction rate varies exponentially with temperature, turbulent temperature fluctuations significantly affect the rate of reaction. Depending on whether the reaction is exothermic or endothermic, the interaction between the chemical reactions and the turbulent flow will give rise to different states of the flow. This has a significant affect on the stability of the flow field. For an endothermic reaction, a temperature fluctuation that causes a rise in temperature will result in an increase in the reaction rate, and consequently, a reduction in temperature. As we show later, this effect tends to stabilize the flow. The opposite will occur in the case of an exothermic reaction.

In this paper, we study the interaction of homogenous isotropic turbulence with chemical reactions at very high temperatures. We use direct numerical simulations (DNS) to solve the Navier-Stokes equations, with additional equations for the conservation of each chemical species. We use a sixth-order accurate finite-difference method based on a compact Padé scheme[1], with fourth-order, low storage Runge-Kutta time integration.

The main objective of this paper is to illustrate the effects of chemical reactions on the turbulent motion. To do so, we introduce the equations of motion of a reacting fluid in section II. In section III, we present the non-dimensional parameters that govern the physical phenomena. In section IV, because of the complexity of the problem, we introduce some simplifications that help isolate the important effects. In section V, we present a range of initial conditions for the direct numerical simulations. Then in section VI, we introduce the results corresponding to the range of initial conditions. And in section VII we conclude with a discussion of the physical phenomena that are caused by the interaction between the turbulence and chemical reactions.

II. Governing Equations

The time-dependent equations describing the motion of a reacting flow with no contribution of vibrational modes are given by the species mass, mass-averaged momentum, and the total energy conservation equations:

$$\frac{\partial \rho_s}{\partial t} + \frac{\partial}{\partial x_j}\left(\rho_s u_j + \rho_s v_{sj}\right) = w_s$$

$$\frac{\partial \rho u_i}{\partial t} + \frac{\partial}{\partial x_j}\left(\rho u_i u_j + p\delta_{ij} - \tau_{ij}\right) = 0$$

$$\frac{\partial E}{\partial t} + \frac{\partial}{\partial x_j}\left[\left(E+p\right)u_j - u_i\tau_{ij} + q_j + \textstyle\sum_s \rho_s v_{sj} h_s\right] = 0 \qquad (1)$$

where w_s represents the rate of production of species s due to chemical reactions; ρ_s is the density of species s; u_j is the mass-averaged velocity in the j direction: v_{sj} is the diffusion velocity of species s; p is the pressure; τ_{ij} is the shear stress tensor given by a linear stress-strain relationship,

$$\tau_{ij} = \mu\left(\frac{\partial u_i}{\partial x_j} + \frac{\partial u_j}{\partial x_i}\right) - \frac{2}{3}\mu\frac{\partial u_k}{\partial x_k}\delta_{ij} \; ; \qquad (2)$$

q_j is the heat flux due to temperature gradients; and h_s is the specific enthalpy of species s; μ is prescribed with a power law $\mu = \mu_\circ\left(\frac{T}{T_\circ}\right)^n$, where $n = 0.7722$, from Gupta et al[2] for the dissociation of N_2, and $\mu_\circ$ is computed from a Sutherland law at 300 K; E is the total energy per unit volume given by:

$$E = \sum_s \rho_s c_{vs} T + \frac{1}{2}\rho u_i u_i + \sum_s \rho_s h_s^\circ \; , \qquad (3)$$

where c_{vs} is the specific heat at constant volume of species s; and h_s° represents the heat of formation of species s.

To derive the expression for w_s, consider a reaction where species S1 reacts to form species S2; the reaction may be symbolically written as:

$$\mathrm{S1} + \mathrm{M} \rightleftharpoons \mathrm{S2} + \mathrm{M} \qquad (4)$$

where M is a collision partner, which is either S1 or S2 in this case. The source terms for S1 and S2 can be written using the law of mass action:

$$\begin{aligned} w_{\mathrm{S1}} = \; & - \; M_{\mathrm{S1}}\, k_f \left(\frac{\rho_{\mathrm{S1}}}{M_{\mathrm{S1}}}\right)\left(\frac{\rho_{\mathrm{S1}}}{M_{\mathrm{S1}}} + \frac{\rho_{\mathrm{S2}}}{M_{\mathrm{S2}}}\right) \\ & + \; M_{\mathrm{S1}}\, k_b \left(\frac{\rho_{\mathrm{S2}}}{M_{\mathrm{S2}}}\right)\left(\frac{\rho_{\mathrm{S1}}}{M_{\mathrm{S1}}} + \frac{\rho_{\mathrm{S2}}}{M_{\mathrm{S2}}}\right) \end{aligned} \qquad (5)$$

and $w_{\mathrm{S2}} = -w_{\mathrm{S1}}$, where k_f and k_b are the forward and backward reaction rates respectively. These are written as:

$$\begin{aligned} k_f &= C_f \; T^\eta e^{-\theta/T} \\ k_b &= k_f / K_{eq} \end{aligned} \qquad (6)$$

K_{eq} is the temperature-dependent equilibrium constant.

For two species, the diffusion velocity can be accurately approximated using Fick's law:

$$\rho_s v_{sj} = -\rho D \frac{\partial c_s}{\partial x_j} \; , \qquad (7)$$

where $c_s = \rho_s/\rho$ is the mass fraction, and D is the diffusion coefficient given in terms of the Lewis number:

$$Le = \frac{D\rho Pr}{\mu} \; , \qquad (8)$$

where Pr is the Prandtl number, $Pr \equiv c_p\mu/k$, and Le is taken to be 1, so that the energy transport due to mass diffusion is equal to the energy transport due to thermal conduction.

III. Assumptions

Because of the complexity of the problem, and for our purposes without loss of generality, we introduced the following assumptions:

We assume a reaction in which the reactants and the products have the same properties. Then S1 and S2 in Eq. 4 have the same molecular weight. With this assumption, the specific heats remain constant, and so does the gas constant.

We assume the following forward rate of reaction:

$$k_f(T) = C \; \frac{\exp\left(-\theta/T\right)}{\exp\left(-\theta/\langle T\rangle\right)} \; , \qquad (9)$$

where $\langle T\rangle$ is the ensemble average of the temperature. With this assumption, we isolate the turbulent effects in the rate of reaction. If there are no turbulent fluctuations, the reaction rate is a constant, C. A positive fluctuation still causes the reaction rate to increase, as described by Eq. 6. Thus, we retain all of the relevant properties of the Arrhenius form of the rate of reaction.

We assume that the equilibrium constant for the reaction is not a function of the temperature. With this assumption, we fix the equilibrium chemical state.

We have compared this model with the real case for the dissociation of nitrogen molecules; and these assumptions do not cause lost of generality.

IV. Governing parameters

In this section, we introduce the non-dimensional numbers governing the physical process. From a non-dimensional analysis the following parameters are obtained: turbulent Mach number, M_t; Reynolds number based on Taylor microscale, Re_λ; Damköhler number, Da; and relative heat release, $\overline{\Delta h^\circ}$. The first

two non-dimensional numbers come from the turbulent state of the flow, and the second two are only present if the flow is chemically reacting:

$$\begin{aligned} M_t &= q \,/\, a \\ Re_\lambda &= \rho u' \lambda \,/\, \mu \\ Da &= \lambda |w_s| \,/\, \rho u' \\ \overline{\Delta h^\circ} &= -\Delta h^\circ \,/\, \left(c_v T + \tfrac{1}{2} q^2\right) \end{aligned} \tag{10}$$

where q is the rms magnitude of the fluctuation velocity; a is the speed of sound; u' is the rms turbulent velocity fluctuation in one direction; $\Delta h^\circ = h^\circ_{S2} - h^\circ_{S1}$ is the heat of the reaction; and c_v is the specific heat at constant volume.

For high levels of M_t and Re_λ, the interaction between the eddy motion and the random noise will be strong, and they will feed each other. At low levels of M_t and Re_λ they are independent of each other.

The Damköhler number is the ratio of the turbulent time scale, τ_t, to the chemical time scale, τ_c, and is directly proportional to the reaction rate.

Finally, $\overline{\Delta h^\circ}$ is the ratio of energy released or absorbed by the chemical process to the internal and kinetic energy. A negative value indicates an endothermic reaction, and a positive value an exothermic reaction. We will see that increasing the values of $\overline{\Delta h^\circ}$ increases the magnitude of the temperature fluctuations, and vice-versa.

V. Numerical Simulations

In this section we present the numerical simulations for three-dimensional, compressible, homogeneous, isotropic, reacting turbulent flow. The numerical method used is based on the method previously used by Lee et al.[3] The simulations were performed on meshes with $(64)^3$, $(96)^3$, and $(128)^3$ points following the criterion given by Reynolds.[4] The computational domain is a periodic box with length 2π in each direction. The velocity field is initialized to an isotropic state prescribed by the following spectrum:

$$E(k) = A\, k^4 \exp\left[-2\left(\frac{k}{k_\circ}\right)^2\right] \tag{11}$$

where A is a proportionality factor that depends on the initial conditions, k are integer non-dimensional wave numbers, and $k_\circ$ is the most energetic wavenumber, which is set equal to 4.

We adopt the same initial conditions used by Lee et al.[3] and include the initial chemistry conditions. We run cases with combinations of $\overline{\Delta h^\circ} = -0.5$, 1.0, 1.5, and 2.0; $Da = 0.5$, 1.0, and 2.0; $M_t = 0.173$, 0.346, and 0.519; and $Re_\lambda = 25.0$, 34.5, and 50.0. We also specify the initial density and temperature as $\rho_\circ = 1.0$ kg/m^3 and $T_\circ = 6462$ K, with zero initial fluctuations. We use S1 = S2 = N, with initial $c_{S1} = 1$ and $c_{S2} = 0$. We choose $K_{eq} = 1$, so that equilibrium is reached when $c_{S1} = c_{S2} = 0.5$.

The chemical reactions are turned off until the initial field has evolved to realistic turbulence. Because the initial field is incompressible, we use values of velocity derivative skewness, S_i, to predict the onset of realistic turbulence. Experimental data presented by Tavoularis et al.[5] and Orszag et al.[6] shows that S_i ranges in $[-0.6 : -0.35]$ for realistic turbulence at Re_λ near 50. All results are presented starting after the turbulence has developed into realistic turbulence.

The following section presents the results from the numerical simulations and illustrates the effect of each of the four governing parameters.

VI. Results

Let us now focus on how the chemical reactions affect the gas dynamics. Consider Figure 1a, which plots the average of the reactant mass fraction for $\overline{\Delta h^\circ} = 1.0$, $Da = 1.0$, $M_t = 0.346$, and $Re_\lambda = 34.5$. We observe that at $t/\tau_t = t/\tau_c = 2.0$, the reactant concentration asymptotically approaches equilibrium.

Due to the exothermic nature of the conditions chosen, the average temperature of the flow increases rapidly for the reacting case. For the non-reacting simulation, the temperature increases slightly as the turbulence decays. This can be seen in Fig. 1b, which plots the average temperature during the reacting and non-reacting simulations for the conditions given above.

Figure 1c plots the temporal evolution of the turbulent kinetic energy. For a period of time of about $t/\tau_t = 0.2$, the turbulent kinetic energy is enhanced by the exothermic chemical reactions. Then in the period of time between [0.2 : 1.75], the turbulent ki-

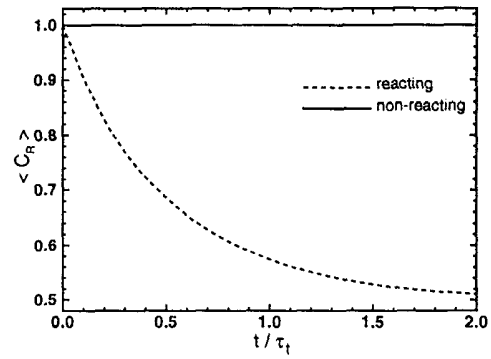

(a)

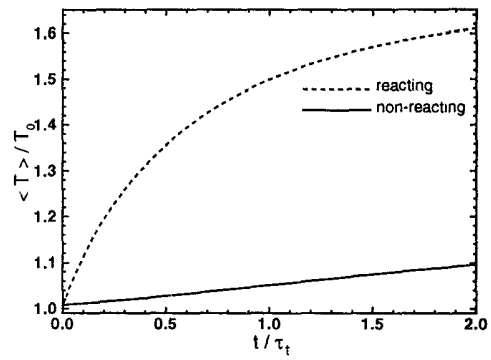

(b)

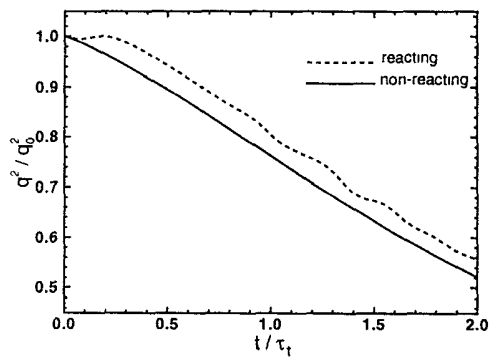

(c)

Figure 1. Time evolutions of reactant mass fraction (a), average temperature (b), and turbulent kinetic energy (c), comparing reacting and non-reacting simulations for $\overline{\Delta h^\circ} = 1$, $Da = 1$, $M_t = 0.346$, and $Re_\lambda = 34.5$.

netic energy decreases slightly faster for the reacting simulation. Note that from Fig. 1a, the reaction rate is fastest up to $t/\tau_t = 0.2$. After that the exothermic reaction is still reaching the chemical equilibrium, but at a slower rate. This means that the rate at which heat is being released into the flow is considerably lower than at the previous time.

Turbulence is dissipative, and it needs a continuous supply of energy to keep from decaying. For homogeneous flow, the dissipation is given by the following expression:

$$\epsilon = \nu \left\langle \left(\frac{\partial u_i}{\partial x_j} + \frac{\partial u_j}{\partial x_i} \right) \frac{\partial u_i}{\partial x_j} \right\rangle - \frac{2}{3} \nu \left\langle \left(\frac{\partial u_i}{\partial x_i} \right)^2 \right\rangle \quad (12)$$

where ν is the dynamic viscosity. Moyal[7] decomposed the velocity field, $\vec{u}(x)$, in Fourier space into solenoidal (divergence-free) $\hat{\vec{u}}^I$, and dilatational (curl-free) $\hat{\vec{u}}^C$ components:

$$\hat{\vec{u}}^I = \hat{\vec{u}} - \frac{\hat{\vec{k}} \cdot \hat{\vec{u}}}{k^2} \vec{k} \quad (13)$$

$$\hat{\vec{u}}^C = \hat{\vec{u}} - \hat{\vec{u}}^I \quad (14)$$

Then the dissipation can be written as:

$$\epsilon = 8\pi\nu \int_0^\infty \left(E^I(k) + \frac{4}{3} E^C(k) \right) k^4 dk \quad (15)$$

where isotropic conditions have been assumed, and where $E^I(K)$ and $E^C(k)$ represent solenoidal (divergence-free) and dilatational (curl-free) components of the energy spectrum:

$$E^C(k) = \frac{1}{2} \hat{\vec{u}}^C(k) \cdot \hat{\vec{u}}^C(k) \quad (16)$$

$$E^I(k) = \frac{1}{2} \hat{\vec{u}}^I(k) \cdot \hat{\vec{u}}^I(k) \quad (17)$$

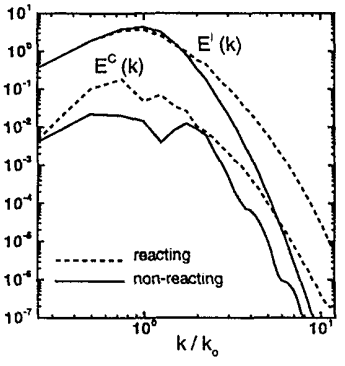

(a)

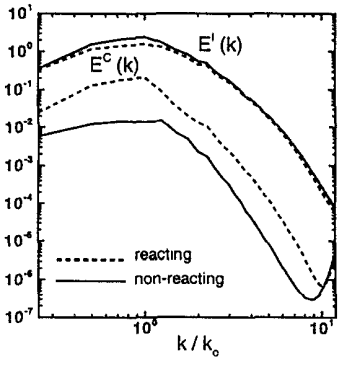

(b)

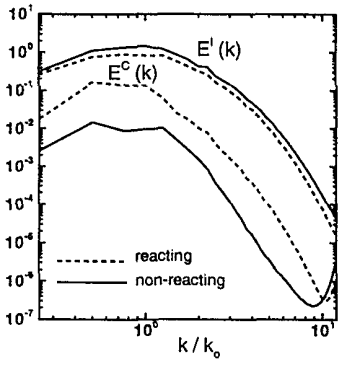

(c)

Figure 2. Three dimensional solenoidal, E^I, and dilatational, E^C, energy spectra showing the effects of chemical reactions for (a) $t/\tau_t = 0.2$, (b) $t/\tau_t = 1.75$, and (c) $t/\tau_t = 3.0$ for $\overline{\Delta h^\circ} = 1$, $Da = 1$, $M_t = 0.346$, and $Re_\lambda = 34.5$ simulation. Non-reacting simulation corresponds to solid line, reacting corresponds to dashed line.

Consider Fig. 2, which plots the energy spectrum for the reacting and non-reacting simulations at $t/\tau_t = 0.2$, 1.75, and 3.0 respectively. From the numerical simulations we observe that in the period of time [0.0:0.2], the energy contained in the compressible modes increases for the reacting simulation. Between $t/\tau_t = 0.2$ and $t/\tau_t = 1.75$, the compressible energy mode increases slightly. After $t/\tau_t = 1.75$, both energy spectra decrease in the large scale range, while increasing in the small scale range in a similar fashion. We observe that the incompressible modes are higher for the reacting case. Also, the compressible modes are more than one order of magnitude larger. From Eq. 15, we see that the dissipation will be higher for the reacting simulation, which accounts for the slightly more rapid decay of the kinetic energy, as seen in Fig. 1c.

The root mean square of the temperature fluctuations, T'_{rms}, also decreases as the species react to form the products. Figure 3 shows the temporal evolution of the rms temperature fluctuations for the reacting and non-reacting simulations. We observe that the temperature fluctuations reach much higher values in the case of the exothermic reaction than in the non-reacting simulation, and then they very slowly decay.

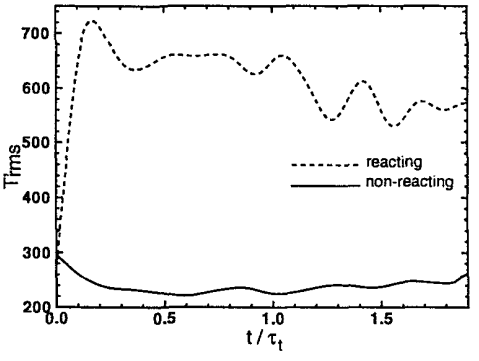

Figure 3. Time evolution of rms temperature fluctuations comparing reacting and non-reacting simulations for $\overline{\Delta h^\circ} = 1$, $Da = 1$, $M_t = 0.346$, and $Re_\lambda = 34.5$.

To explain the behavior of these fluctuations, we introduce the linearized form of Eq. 9:

$$k_f = C\left(1 + \frac{\theta\, T'}{\langle T\rangle^2}\right) \tag{18}$$

A positive temperature fluctuation causes an increase in the source term, and vice versa. From this expression, it can be deduced that as the rate of reaction slows down and the formation of products decreases, temperature fluctuations will slowly decrease towards a quasi steady value.

A. Relative Heat Release Results

In the following results we illustrate the effects of the variations of the relative heat release for moderated Da, M_t, and Re_λ, namely $Da = 1$, $M_t = 0.346$, and $Re_\lambda = 34.5$. Consider Fig. 4, which plots the temporal evolution of the average temperature in time. As we increase the exothermicity of the reaction, the average temperature increases towards a higher equilibrium value.

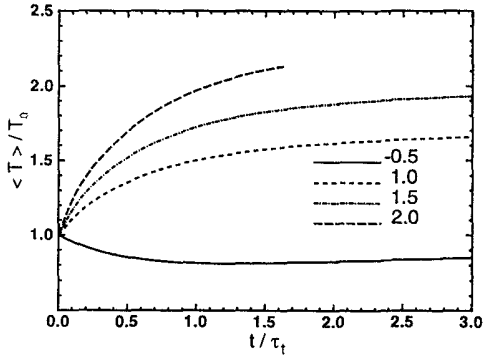

Figure 4. Time evolutions of average temperature showing the effects of $\overline{\Delta h^\circ}$ for $Da = 1$, $M_t = 0.346$, and $Re_\lambda = 34.6$.

As the relative heat released into the flow is increased, the turbulent kinetic energy decays more slowly. Figure 5a plots the temporal evolution of turbulent kinetic energy for the different exothermic reactions. It should be noted that when $\overline{\Delta h^\circ} = 1$, there is an initial period of time when the turbulence is enhanced. When the initial relative heat release is increased farther, the turbulent kinetic energy is considerably enhanced, maintaining and feeding the turbulence.

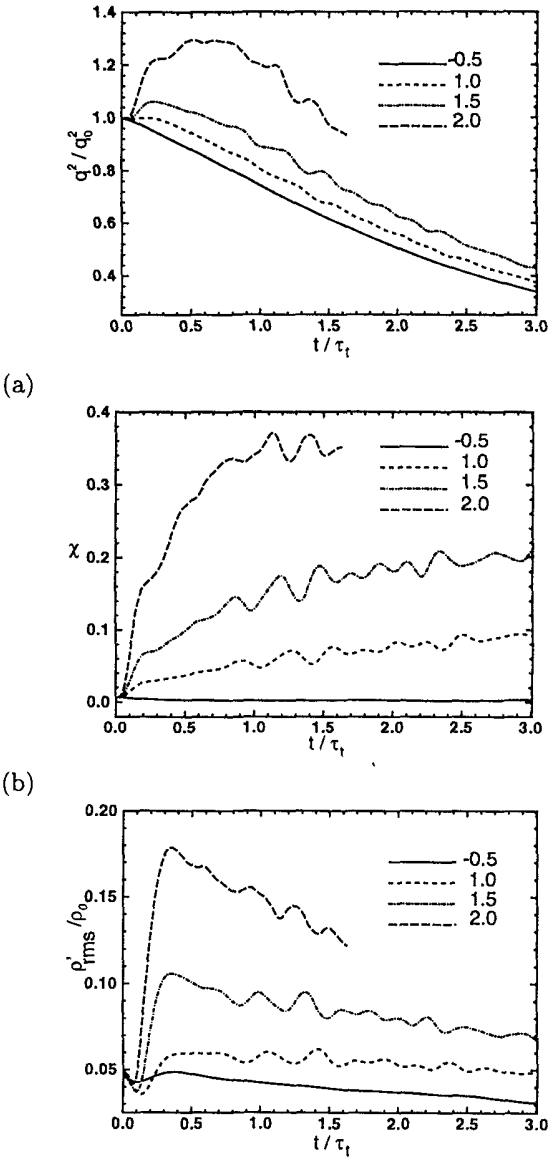

Figure 5. Time evolutions of turbulent kinetic energy (a), relative compressible kinetic energy χ (b), and rms density fluctuations (c) showing the effects of $\overline{\Delta h^\circ}$ for $Da = 1$, $M_t = 0.346$, and $Re_\lambda = 34.5$.

Figure 5b shows the evolution of the relative compressible energy, ratio χ:

$$\chi = \frac{\int \vec{u}^C \cdot \vec{u}^C \, d\vec{x}}{\int \vec{u}^C \cdot \vec{u}^C + \vec{u}^I \cdot \vec{u}^I \, d\vec{x}} \qquad (19)$$

The initial value of χ is very low, and for the case of endothermic reaction, χ remains very small as the turbulence evolves in time. For $\overline{\Delta h^\circ} = 1.0$, the relative compressible kinetic energy increases to 10% at $t/\tau_t = 3.0$. For $\overline{\Delta h^\circ} = 1.5$, χ increases up to 21%. A further increase in the relative heat release to $\overline{\Delta h^\circ} = 2.0$ causes χ to increase rapidly, reaching 35% of the total kinetic energy at about $t/\tau_t = 1.1$.

This enhancement of compressibility is reflected in the rms fluctuations in density as shown in Fig. 5c. For the case of an endothermic reaction, the fluctuations in density are damped from their original value. As the heat release is increased, the fluctuations in density increase, indicating an increase of compressibility in the flow.

Consider the energy spectrum of the flow field decomposed into its dilatational (curl-free) and solenoidal (divergence-free) components at different times. In Fig. 6a, we observe that the compressible modes are about three orders of magnitude less energetic than the incompressible modes for the non-reacting case. As time evolves, the compressible energy spectrum remains nearly the same, whereas the incompressible modes decrease in the large scale range, and increase in the small scale range as the turbulence decays.

Figure 6b shows the spectra for the endothermic simulation. The compressible modes are still three orders of magnitude below the incompressible modes. As time evolves, they decrease further over all scales. The incompressible modes decrease slightly more in the large scale range for the endothermic case than in the non-reacting case. Figure 6c plots the energy spectra for $\overline{\Delta h^\circ} = 1$. The compressible modes are about one order of magnitude higher in this case than in the non-reacting case. However, the incompressible modes preserve the same characteristics in the large scale range as the non-reacting simulation. In the range of small scales, the incompressible modes increase through a period of time $t/\tau_t = 0.3$, after that they remain nearly constant.

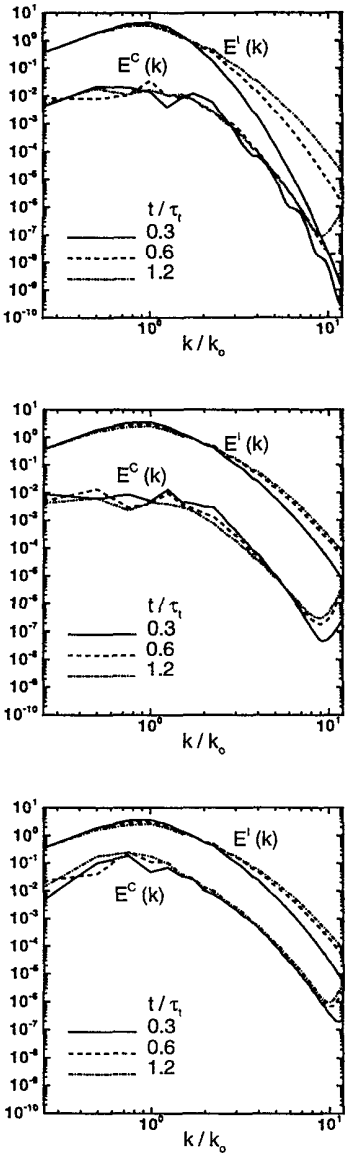

Figure 6. Three dimensional solenoidal, E^I, and dilatational, E^C, energy spectra showing the effects of the initial relative heat released for the case of Fig. 5, for non-reacting simulation (a), $\overline{\Delta h^\circ} = -0.5$ simulation (b), and $\overline{\Delta h^\circ} = 1$ simulation (c). The values of t/τ_t correspond to 0.3 solid line, 0.6 dashed line, 0.9 dash-dotted line and 1.2 dotted line.

Consider Figure 7, which plots the three dimensional dilatational and solenoidal energy spectra, for $\overline{\Delta h^\circ} = 2$ at various times. The compressible modes increase by another order of magnitude with respect to the previous case, almost reaching the incompressible modes in the large scale range. The compressible modes are dominant in the small scale range.

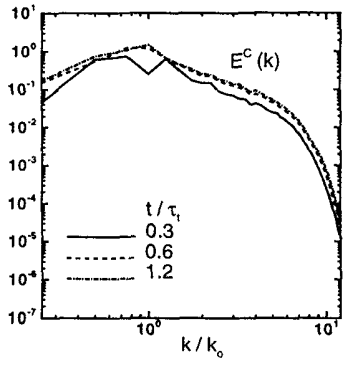

(a)

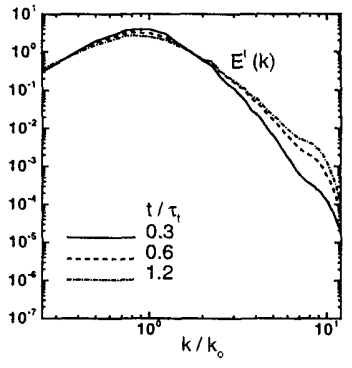

(b)

Figure 7. Three dimensional dilatational, E^I (a) and solenoidal, E^C (b) energy spectra showing the effects of the initial relative heat release for $\overline{\Delta h^\circ} = 2$ with $Da = 1$, $M_t = 0.346$, and $Re_\lambda = 34.5$. The values of t/τ_t correspond to 0.3 solid line. 0.6 dashed line, 0.9 dash-dotted line and 1.2 dotted line.

In Figure 8 we observe a remarkable increase in the magnitude of the temperature fluctuations when the heat release is increased. Because the magnitude of T'_{rms} increases as we increase the exothermicity of the reaction, the reaction rate increases. After equilibrium has been reached the magnitude of T'_{rms} is nearly maintained for the exothermic simulations. For the endothermic case, T'_{rms} decreases initially and then increases to a nearly steady value.

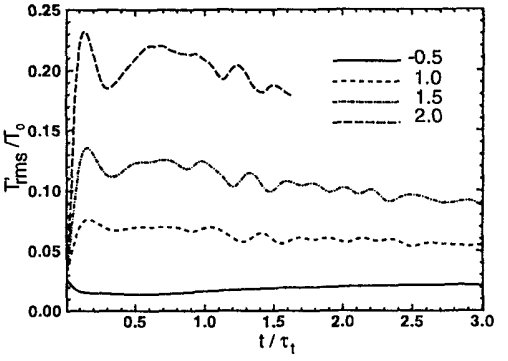

Figure 8. Time evolution of rms temperature fluctuations showing the effects of $\overline{\Delta h^\circ}$ for $Da = 1.0$, $M_t = 0.346$, and $Re_\lambda = 34.5$.

B. Damköhler Number Results

The Damköhler number is the ratio of the turbulent time scale to the chemical time scale. Therefore, an increase in Da will cause an increase in the reaction rate, which in itself causes more rapid heat release if the reaction is exothermic. Therefore, as Da increases we expect that the species will reach chemical equilibrium in a shorter time. To illustrate the effects of the Damköhler number, we consider a case of moderate heat release, turbulent Mach number, and Reynolds number, namely $\overline{\Delta h^\circ} = 1$, $M_t = 0.346$, and $Re_\lambda = 34.5$.

Consider Fig. 9a, which shows the temporal evolution of the average concentration of reactant species. We observe that the reactants asymptotically aproach equilibrium at $t/\tau_t = 2.0$, and 1.0 for $Da = 1.0$, and 2.0 respectively. The simulation corresponding to $Da = 0.5$ has not reached chemical equilibrium at $t/\tau_t = 3.0$.

Figure 9b plots the evolution of the turbulent kinetic energy. Initially, for a short period of time, the turbulence is enhanced with increased Da. However, as time evolves, the kinetic energy decay is slightly faster for higher values of Da. This is due to an increase in the dissipation due to compressibility effects. See Eq. 15. The three simulations reach nearly the same value of $(q/q_o)^2$ at $t/t_\tau = 3.0$. Figure 9c

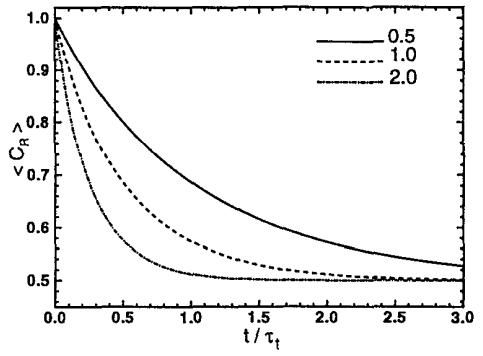

(a)

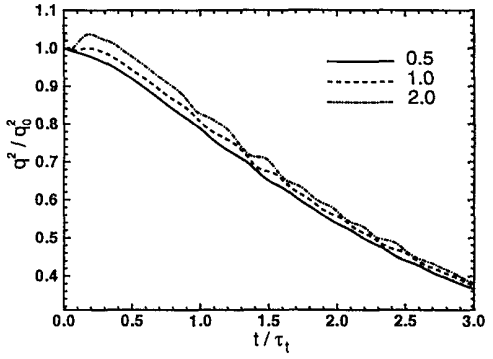

(b)

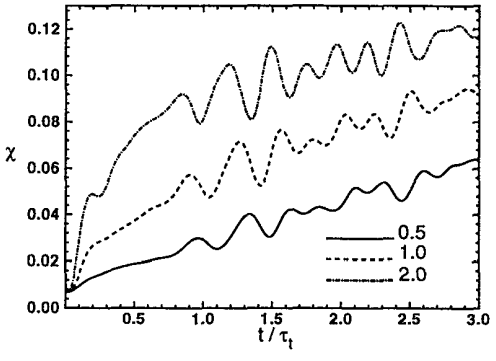

(c)

Figure 9. Time evolutions of averages of the average concentration of reactants (a), turbulent kinetic energy (b), and relative compressible energy, χ (c) showing the effect of the initial Damköhler number for $\overline{\Delta h^\circ} = 1$, $M_t = 0.346$, and $Re_\lambda = 34.5$.

plots the relative compressible kinetic energy, χ. The compressibility in the flow field increases as we increase the initial Damköhler number. Also note that the magnitude of the temporal fluctuations in χ increases with Da, showing a form of feedback between heat release and fluid dynamic fluctuation.

Because of the proportionality between T'_{rms} and k_f, see Eq. 18, the larger the turbulent temperature fluctuations the more exothermic reaction that will take place, and vice versa. Figure 10 illustrates the effects of the Damköhler number for the same simulation as the one shown in Fig. 9. As Da increases, T'_{rms} reaches a larger value.

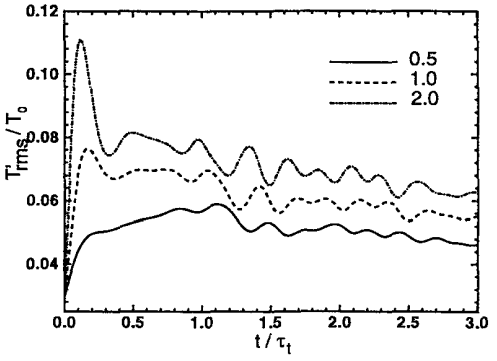

Figure 10. Time evolution of rms temperature fluctuations showing the effect of the initial Damköhler number for $\overline{\Delta h^\circ} = 1$, $M_t = 0.346$, and $Re_\lambda = 34.5$.

C. Turbulent Mach Number Results

To describe the effects of the turbulent Mach number, we choose a case of moderate Damköhler number, relative heat release, and Reynolds number, namely $\overline{\Delta h^\circ} = 1$, $Da = 1$, and $Re_\lambda = 34.5$.

Our results show no effect of M_t on the rate of reaction. Figure 11a plots the temporal evolution of the average temperature. As the initial turbulent Mach number is increased, the average temperature reaches higher values because more kinetic energy is dissipated and converted to internal energy. For the same simulations, Fig. 11b shows the decay of kinetic energy. For $M_t = 0.346$, the turbulence is enhanced initially until $t/\tau_t = 0.2$. The same characteristic is observed for the case of $M_t = 0.519$, where the turbulence is enhanced even more than in the previous

case until $t/\tau_t = 0.28$. After that, and for all cases, the kinetic energy decays. It appears that the higher the initial Mach number, the steeper the decay will be.

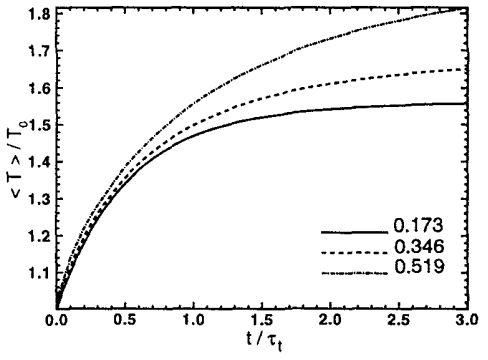

(a)

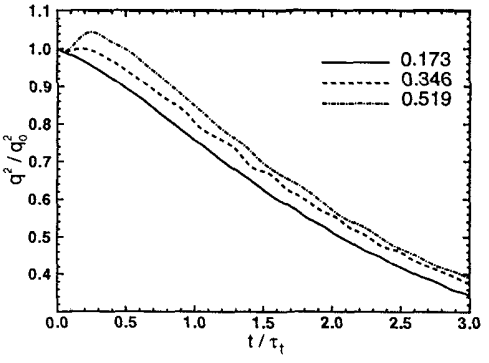

(b)

Figure 11. Time evolutions of average temperature (a), and turbulent kinetic energy (b) showing the effects of initial Mach number variations for $\overline{\Delta h^\circ} = 1$, $Da = 1$, and $Re_\lambda = 34.5$.

As expected, the compressibility of the flow increases for higher initial Mach number simulations. Figure 12 plots the evolution of the relative compressible energy, χ, for the simulations described above. Figure 13 shows the solenoidal and dilatational components of the energy spectra at $t/\tau_t = 1.75$. While the incompressible modes contain similar characteristics for the three simulations, the compressible modes are enhanced over all scales for higher initial turbulent Mach numbers.

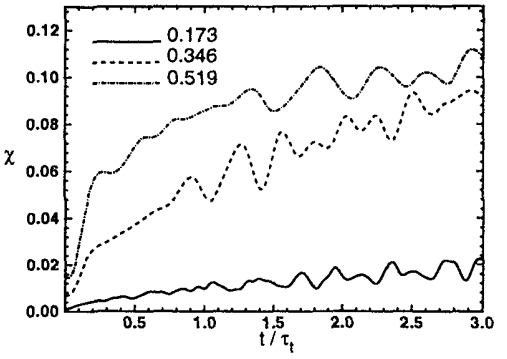

Figure 12. Time evolution of relative compressible kinetic energy, χ, showing the effects of initial Mach number variations for $\overline{\Delta h^\circ} = 1$, $Da = 1$, and $Re_\lambda = 34.5$.

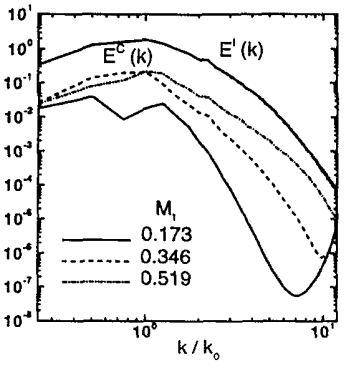

Figure 13. Three dimensional solenoidal, E^I, and dilatational, E^C, energy spectra showing the effects of initial Mach number variations for $\overline{\Delta h^\circ} = 1$, $Da = 1$, and $Re_\lambda = 34.5$ at $t/\tau_t = 1.75$.

Finally, consider Figure 14 which plots the temporal evolution of the rms temperature fluctuations. We observe that for higher initial Mach numbers, the rms temperature fluctuations are higher at $t/\tau_t = 0.0$, and the reacting process begins, T'_{rms} increases. Then, as chemical equilibrium is reached, T'_{rms} settles down to a quasi steady value.

D. Reynolds Number Results

From the direct numerical simulations we concluded that the is very little effect due to different

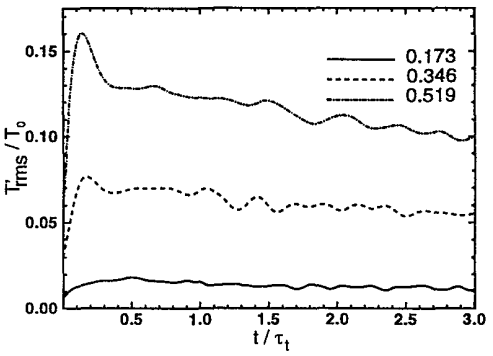

Figure 14. Time evolution of the rms temperature fluctuations showing the effects of initial Mach number variations for $\overline{\Delta h^\circ} = 1$, $Da = 1$, and $Re_\lambda = 34.5$.

initial Reynolds numbers. We observe no variation in the rate of reaction. Due to the smaller dissipation of a higher Reynolds number simulation, the temperature increases more slowly. The rms temperature fluctuations reach higher values as we increase the Reynolds number. This must also be due to the lower dissipation in the flow. The increase in the compressibility of the flow is almost negligible.

VII. Discussion

The different effects of the independent initial parameters that govern the interaction process between the turbulent motion and the chemical reactions have been described in the previous section. The two most striking characteristics of the interaction are the large increase in the rms temperature fluctuations and the large increase in the compressibility of the flow, caused by increases in the exothermicity of the reaction. As mentioned previously, a positive turbulent temperature fluctuation causes an increase in the reaction rate and vice versa. From these results we can conclude that a physical mechanism with feedback between the turbulence and the chemical reactions takes place. As shown, the feedback is positive for exothermic reactions, and negative for endothermic reactions. In the following, we discuss the physical mechanism that takes place in the flow field.

A. Interaction Mechanism

To explain the physical phenomena driving the interaction between the turbulent motion and the chemical reactions, we must address three issues: (1) the maintenance of the turbulent motion due to the heat released to the flow; (2) the explanation of the appearance of density, and pressure fluctuations in the turbulent motion; and (3) the magnification of temperature fluctuations due to the feedback process between the turbulent motion and the chemical reactions. The first two issues are explained in this section. Because of the importance of the third issue, it is left to be explained in the next subsection.

We have corroborated the theoretical results of Eschenroeder[8] that the turbulent motion is fed from the external source of energy provided by exothermic reactions. Our results show that: the heat released into the flow is converted into turbulent kinetic energy through the dilatational modes of motion, the reactions are independent of the turbulent scale, and the reactions are enhanced in regions of high compression since the temperature increases there.

The energy produced by the chemical reaction acts in the flow field as pressure work. Because the flow is turbulent, some spots are hotter than others. Due to the different temperature fluctuations present in the flow field, more or less reaction occurs depending location in the flow field. This further enhances the temperature and therefore the pressure in hot spots. This causes expansions and compressions through the flow field. In this way, some of the internal energy produced by the chemical reactions is converted into kinetic energy through the dilatational turbulent motion. This addition of compressibility is reflected in the fluctuations of density and pressure.

The fact that there is not a direct influence of the external energy source due to the chemical reactions on the solenoidal part of the motion, can be seen by studying the vorticity equation. The direct influence is embedded in the vorticity production due to thermodynamic changes in the flow:

$$-\tfrac{1}{\rho^2}\left(\nabla P \times \nabla \rho\right) = \begin{array}{l}(\nabla T \times \nabla S_i) - \\ (\nabla T \times \sum_s S_s \nabla c_s)\end{array} \qquad (20)$$

where S_i is the entropy associated with changes in the thermodynamic state, and where S_s is the entropy associated with the formation or destruction of

species s, namely:

$$S_s = \frac{h_s^\circ}{T} M_s - \mu_s^\circ M_s \tag{21}$$

h_s° is the standard heat of formation of species s, M_s is the molecular weight of species s, and μ_s° is the chemical potential for the reaction. The influence of the chemical heat release is subtracted from the production of vorticity. Greenberg[9] deduced that due to the symmetry of the problem, the second term in Eq. 20 does not contribute to the production of vorticity. And therefore, the indirect contribution to vorticity from the chemical heat release must be in the vortex stretching and turning terms and in the production of vorticity due to compressibility effects in the vorticity equation. Our results agree with this statement. However, the gradients of temperature and species concentration will be parallel to one another if the flow is in chemical equilibrium. But if the flow is in non-equilibrium, there will be a time lag between the gradients of temperature and species concentration. Therefore, these vectors will not necessarily be parallel, adding some asymmetry to the problem. We need to further study the influence of this term on the vorticity production.

B. Temperature Fluctuations

The magnitude of the temperature fluctuations is strongly affected by the the rate of reaction, and the amount of heat released into the flow. To explain the dependence on the first factor, consider Eq. 18. The reaction rate is proportional to the temperature fluctuations. In the case of an exothermic reaction, a positive turbulent fluctuation will cause an increase in the rate of reaction. This in effect causes more turbulent fluctuations in density and pressure as explained previously. Then, through the thermodynamic state balance, the temperature fluctuations are further increased. This constitutes a physical mechanism with positive feedback between the chemical reactions and the turbulent fluctuations.

For high levels of heat release, the level of compressibility increases. Therefore, the magnitude of the temperature fluctuations is increased as well. As the gas reaches chemical equilibrium, the amount of energy that is being removed is the same as the amount of energy that is being released into the flow.

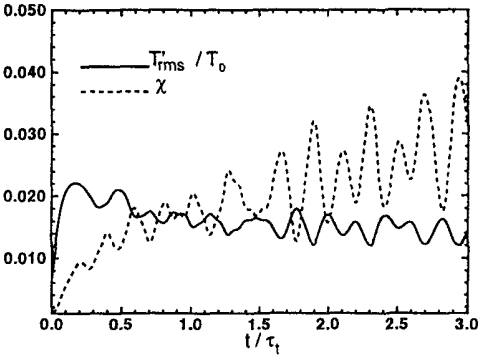

(a)

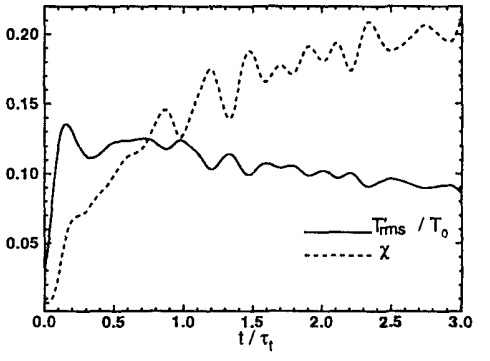

(b)

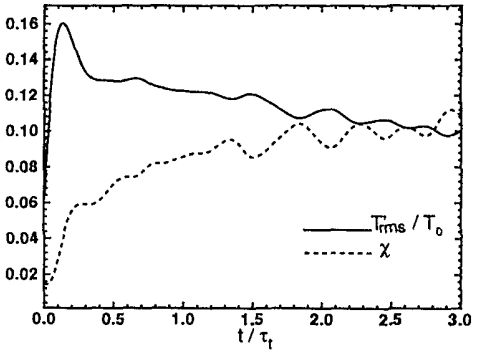

(c)

Figure 15. Time evolutions of normalized fluctuating internal energy and relative compressible kinetic energy showing the effect of chemical reactions in the exchange of turbulent energy for $\overline{\Delta h^\circ} = 1$, $Da = 2$, $M_t = 0.173$, and $Re_\lambda = 34.5$ (a), $\overline{\Delta h^\circ} = 1.5$, $Da = 1$, $M_t = 0.346$, and $Re_\lambda = 34.5$ (b), and $\overline{\Delta h^\circ} = 1$, $Da = 1$, $M_t = 0.519$, and $Re_\lambda = 34.5$ (c).

At this point, the amplitude of the temperature oscillations remains nearly constant.

The energy released into the flow due to the chemical reactions increases the local temperature, and as a result increases the local pressure. These pressure fluctuations are converted to kinetic energy through the reversible work term, $p\nabla \cdot \vec{u}$ in the energy equation. They have a characteristic period; in time units normalized by the turbulent time scale, this period is proportional to the Mach number. Therefore, the fluctuations in density, pressure, and temperature propagate as acoustical waves through the three-dimensional periodic box.

Because the internal energy increases continuously with time, it is difficult to observe the equipartition between the kinetic energy and the internal energy, that would be present if the reversible work term was responsible for the conversion of local temperature fluctuations. However, if we study the ratio of the compressible kinetic energy to the normalized fluctuating internal energy, we observe an equipartition of energy. Consider Fig. 15, which plots the temporal evolutions of the normalized fluctuating internal and compressible kinetic energies for three different simulations. In all cases, we observe that the fluctuating internal energy and compressible energy oscillate in phase. Therefore, the chemistry does reversible work on the turbulence. This agrees with the previous explanation that due to the temperature fluctuations some of the internal energy is converted into compressible kinetic energy.

This feedback process may have major importance in reacting turbulent boundary layers. In the case of a cold or catalytic wall, exothermic reactions such as the one considered here occur. Under any small perturbation of the flow field, this physical mechanism will generate and feed itself, enhancing the turbulence and chemical effects (and potentially destabilizing the flow in the boundary layer). The above discussion also applies to the case of endothermic reactions, where the feedback is negative, and therefore stabilizing.

VIII. Conclusion

In this paper we consider how finite rate reactions interact with homogeneous, isotropic turbulence. We find that there is a feedback mechanism between the turbulence and the chemistry. In the case of exothermic reactions, temperature fluctuations increase the reaction rate, which increases the rate of energy released to the flow. This increases the temperature, and through the equation of state, the pressure. The higher temperature causes the reaction rate to be further increased, and the increased pressure causes the gas to expand. This results in energy transfer from the internal energy to the kinetic energy, increasing the dilatational modes of the turbulent motion. We see clear evidence of the process through increased levels of the rms temperature fluctuation and fraction of the kinetic energy in the compressible modes. It is important to note that the simulations with exothermic reactions show dramatically increased levels of energy at high wavenumbers, indicating that the heat release increases the turbulent energy in a scale-independent fashion. These effects are reverse for endothermic reactions.

Acknowledgments

We would like to acknowledge support from the Air Force Office of Scientific Research. This work was also sponsored by the Army High Performance Computing Research Center under the auspices of the Department of the Army, Army Research Laboratory cooperative agreement number DAAH04-95-2-0003 / contract number DAAH04-95-C-0008, the content of which does not necessarily reflect the position or the policy of the government, and no official endorsement should be inferred. Computer time was provided by the University of Minnesota Supercomputer Institute.

References

[1] S.K. Lele. Compact finite difference schemes with spectral-like resolution. *Journal of Computational Physics*, 103:16–42, August 1991.

[2] R.N. Gupta, J.M. Yos, R.A. Thompson, and K. Lee. A review of reaction rates and thermodynamic and transport properties for an 11-species air model for chemical and thermal nonequilibrium calculations to 30000 k. *NASA Reference Publication*, page 1232, 1990.

[3] S. Lee, S.K. Lele, and P. Moin. Eddy-shocklets in decaying compressible turbulence. *Phys. Fluids A*, 3(4):657–664, April 1991.

[4] W.C. Reynolds. The potential and limitations of direct and large eddy simulations. *Whither Turbulence, Lecture Notes in Physics*, 357:313–343, 1991.

[5] S. Tavoularis, J.C. Bennett, and S. Corrsin. Velocity derivative skewness in small reynolds number nearly isotropic turbulence. *Journal of Fluid Mechanics*, 88:63–69, February 1978.

[6] S.A. Orszag and G.S. Patterson. Numerical simulation of three dimensional homogeneous isotropic turbulence. *Physical Review Letters*, 28(2):76–79, January 1972.

[7] J.E. Moyal. The spectra of turbulence in a compressible fluid; eddy turbulence and random noise. *Proc. Cambridge Phil. Soc.*, 48:329–344, April 1951.

[8] A.Q. Eschenroeder. Intensification of turbulence by chemical heat release. *Physics of Fluids*, 7(11):1735–1741, November 1964.

[9] R. A. Greenberg. Non-equilibrium vortex flow in a dissociating gas. *Journal of the Aerospace Sciences*. 29:1484–1485, December 1962.